

# On Approximation of Human Corneal Surface with Superellipsoids

M. Talu<sup>1</sup>, S. Talu<sup>2</sup>, S.D. Talu<sup>3</sup>, and R. Shah<sup>4</sup>

<sup>1</sup> Faculty of Mechanics / Department of Applied Mechanics, University of Craiova, Romania

<sup>2</sup> Faculty of Mechanics / Department of Descriptive Geometry and Engineering Graphics, Technical University of Cluj-Napoca, Romania

<sup>3</sup> Faculty of Medicine / Department of Ophthalmology, "Iuliu Hatieganu" University of Medicine and Pharmacy Cluj-Napoca, Romania

<sup>4</sup> Massachusetts Eye Research and Surgery Institution, Boston, Massachusetts, U.S.A.

**Abstract**— The objective of this paper is to present results of the theoretical and experimental researches for determination of an approximation of human corneal surface with superellipsoids using computational geometry. The mathematical formula permits a complex representation and the tool allowing exploring the physical and optical characteristics of the cornea. The spatial shape of the cornea can be described using different mathematical models with particular parameters for different subjects (women and men). These researches are applied in geometric constructions and computer aided design used in corneal refractive surgery, human vision studies, solid modelling and biomechanical behavior of the cornea.

**Keywords**— human corneal surface, superellipsoids, computational geometry.

## I. INTRODUCTION

The ophthalmology has benefited from computational methods in computer graphics, used for evaluation of patient data [1].

The visual analyzer is a complex system that has the purpose to receive, analyze and synthetize the informations regarding the shape, the dimension, the colour, the movement and the spatial depth of the objects in the surrounding area (Fig. 1).

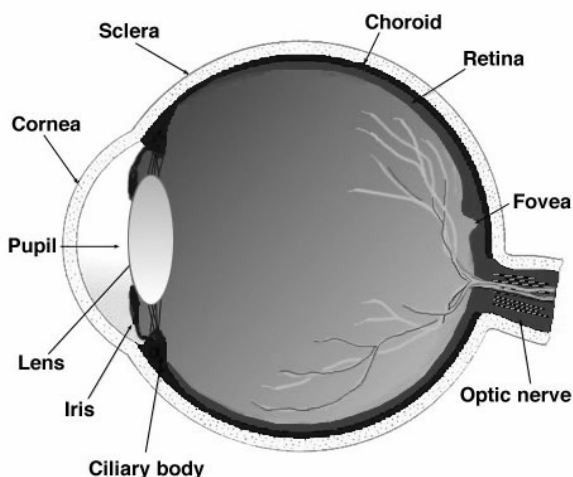


Fig. 1 The human eye – traverse section

The accurate measurement of corneal shape, refractive power and thickness has become important with the continuously growing popularity of refractive surgery procedures. Also, exact measurement of the corneal curvature is essential to properly fit contact lenses [1, 2].

Corneal topography is a modern invaluable tool to assist in the diagnosis and management of keratoconus as well as for the prevention of inappropriate refractive surgery in the patient groups [3 -10].

The cornea is the transparent front part of the eye that covers the iris, pupil, and anterior chamber (placed between air and aqueous humour), providing most of an eye's optical power, with a refraction index of 1.376. The refractive power of the cornea is approximately 43 dioptres, roughly two-thirds of the eye's total refractive power [11 – 21].

The central dioptric power of the cornea (43 dioptres) results from the addition of the dioptric powers of the three optical interfaces (air - tear film = + 43.6 D, tear film - cornea = + 5.3 D, cornea - aqueous humor = - 5.8 D).

The cornea presents the typical aspect of a divergent meniscus, in contact with transparent media having different refractive indices.

Cornea is a transparent and refractive tissue having a fixed curvature. Because transparency is of prime importance the cornea does not have blood vessels; it receives nutrients via diffusion from the tear fluid at the outside and the aqueous humour at the inside and also from neurotrophins supplied by nerve fibres that innervate it.

The adult cornea is normally clear, has a uniform surface, and is comprised of five layers: epithelium, Bowman's membrane, stroma, Descemet's membrane and the endothelium.

The corneal shape is maintained by its elastic properties in conjunction with intraocular pressure, generated by the continuous production and outflow of aqueous humor in the eye.

The adult cornea has a diameter of about 11.5 mm and a thickness of (0.5 - 0.6) mm in the center and (0.6 - 0.8) mm at the periphery.

The normal cornea has an aspheric profile that is more steeply curved in the center relative to the periphery.

The cornea is transparent for radiations comprised between (400 - 760) nm.

The transparency is influenced by anatomical and biochemical factors, such as: the regularity of the cells, the parallelism of the fibers, the absence of the blood vessels.

From the biochemical point of view, the transparency depends on the hydration, which is around 80 %. Transparency, avascularity, and immunologic privilege makes the cornea a special tissue.

To model the eye as an optical system it is necessary to describe of the anterior and the posterior corneal surfaces.

The aim of human corneal modelling is to determine the geometrical shape of the corneal surface using algorithms, to convert the input information to a mathematical description of the corneal surface.

The anterior corneal surface has been frequently described in the literature, as it can be measured by widely available techniques [11 – 20]. However, the literature provides only limited data on the posterior corneal surface [14, 15]; asphericity information is particularly scarce.

The asphericity of the posterior cornea has been measured by different authours using a combined approach involving a keratoscope to measure the anterior corneal surface and pachymetry to measure the thickness profile of the cornea [2, 13, 15, 21].

## II. MATHEMATICAL MODEL

### A. Theoretical Considerations

The mathematical and computer models provide important possibilities that are not available in the experimental studies, which make it to be a useful supplement to experimental studies of the human cornea.

In recent years, superellipsoids have received significant attention for object modeling with their simple and flexible shape description and efficient computer graphical representation, having an important potential for the 3D objects modeling [22, 23, 24]. Using a superellipsoid makes it easy to create simple 3d primitives.

This type of implicit surface can represent various shapes to a high level of accuracy and allows the user to benefit from a generic graphics library, with the implementation of user objects or modules for specific applications.

A superellipsoid, as an ellipsoid's extension, is the result of the spherical product of two 2D models (two superellipses) [22].

A superellipse, analogous to a circle, can be expressed using next relation:

$$\left(\frac{x}{a}\right)^{2/\varepsilon} + \left(\frac{y}{b}\right)^{2/\varepsilon} = 1, \quad a > 0, b > 0. \quad (1)$$

and can be written in next form:

$$s(\theta) = \begin{bmatrix} a \cos^{\varepsilon} \theta \\ b \sin^{\varepsilon} \theta \end{bmatrix}, \quad -\pi \leq \theta \leq \pi. \quad (2)$$

where exponentiation with  $\varepsilon$  is a signed power function such that:

$$\cos^{\varepsilon} \theta = \text{sign}(\cos \theta) |\cos \theta|^{\varepsilon}. \quad (3)$$

Superellipsoids can be expressed by a spherical product of a pair of such superellipses:

$$\begin{aligned} r(\eta, \omega) &= s_1(\eta) \otimes s_2(\omega) = \begin{bmatrix} \cos^{\varepsilon_1} \eta \\ a_3 \sin^{\varepsilon_1} \eta \end{bmatrix} \otimes \begin{bmatrix} a_1 \cos^{\varepsilon_2} \omega \\ a_2 \sin^{\varepsilon_2} \omega \end{bmatrix} = \\ &= \begin{bmatrix} a_1 \cos^{\varepsilon_1} \eta \cos^{\varepsilon_2} \omega \\ a_2 \cos^{\varepsilon_1} \eta \sin^{\varepsilon_2} \omega \\ a_3 \sin^{\varepsilon_1} \eta \end{bmatrix}, \quad -\frac{\pi}{2} \leq \eta \leq \frac{\pi}{2}; \quad -\pi \leq \omega \leq \pi. \end{aligned} \quad (4)$$

The  $a_1, a_2, a_3$  parameters are scaling factors along the three coordinate axes.  $\varepsilon_1$  and  $\varepsilon_2$  are derived from the exponents of the two original superellipses.

This flexibility achieved by raising each trigonometric term to an exponent is of particular interest to us. In simple terms, these exponents, control the relative roundness and squareness in both the horizontal and vertical directions.

The shape of the superellipsoid cross section parallel to the  $[xoy]$  plane is determined by  $\varepsilon_1$ , while the shape of the superellipsoid cross section in a plane perpendicular to the  $[xoy]$  plane and containing  $z$  axis is determined by  $\varepsilon_2$ .

A superellipsoid is defined as the solution of the general form of the implicit equation [23]:

$$\left( \left( \frac{x}{a_1} \right)^{2/\varepsilon_2} + \left( \frac{y}{a_2} \right)^{2/\varepsilon_2} \right)^{\varepsilon_2/\varepsilon_1} + \left( \frac{z}{a_3} \right)^{2/\varepsilon_1} = 1. \quad (5)$$

All points with coordinates  $(x, y, z)$  that correspond to the above equation lie on the surface of the superellipsoid. This is a compact model defined by only five parameters that permits to handle a large variety of shapes.

The exponent functions are continuous to ensure that the superellipsoid model deforms continuously and thus has a smooth surface.

This form provides an information on the position of a 3D point related to the superellipsoid surface, that is important for interior/exterior determination [24].

We have an inside-outside function  $F(x, y, z)$ :

$F(x, y, z) = 1$  when the point lies on the surface;  
 $F(x, y, z) < 1$  when the point is inside the superellipsoid;  
 $F(x, y, z) > 1$  when the point is outside.

### III. MATERIALS AND METHODS

In this section we present a description of our dataset and a summary of the experiments performed.

Based on the experimental research and the statistical analysis, we consider the examination data obtained in our previous work [25].

Gender distribution and age distribution by gender don't differ significantly and therefore possible age dependencies are not influenced by gender [25].

These measurements were performed in order to be able to investigate a possible statistical deviation.

The average radius of the anterior corneal surface was  $7.85 \pm 0.25$  mm. The average radius of the posterior corneal surface was  $6.45 \pm 0.20$  mm. The ratio between the posterior and the anterior radius of curvature was  $0.82 \pm 0.02$ . Mean corneal thickness was  $0.572 \pm 0.032$  mm [25].

We proposed a method that permits an anatomical correspondence between the original data and the created model. This allows us to visualize both textual information and imaging data of our classification results, aiding in clinical decision support.

The computational geometric analyses in this paper are based on the use of the Wolfram CDF Player 8.0 application for computation that generated the 3D superellipsoids [26, 27]. The choice of the geometrical formulation used in the analysis was chosen to ensure that the performance of the model is satisfactory and also to avoid errors associated with modeling materials.

Multiple view range images were used to capture data for the entire surface of the superellipsoid.

To test the geometrical computation the parameters for superellipsoids were chosen for the anterior corneal surface.

The determined parameters for the approximation of human corneal surface with superellipsoids are:

$$a_1 = a_2 = a_3 = 1; \varepsilon_1 = 1, \varepsilon_2 = 0.8 \dots 1.8.$$

The fitting of contour points to the superellipsoid was evaluated by a defined distance measure using the inside-outside function [28, 29]:

$$E = \frac{1}{n} \sum_{i=1}^n (\sqrt{a_1 a_2 a_3} (1 - F^{\varepsilon_1}(x_i, y_i, z_i)))^2 \quad (6)$$

where  $(x_i, y_i, z_i)$  are the detected contours points.

Because the error function is nonlinear the problem of fitting given contour points to superellipsoid model is a nonlinear estimation problem.

We used the Levenberg-Marquardt algorithm [30, 31, 32] which solves nonlinear least square minimization of the error function.

In this case it is necessary to input a set of initial values. We considered that the origin of object-centered coordinate

system is aligned to the center of gravity of all the  $n$  contour points. The distance between the outermost contour points along each coordinate axis of the object-centered coordinate system is the site of initial fitting curve.

If it is increased the surface model, it is possible to capture the surface irregularities that distinguish between the different data. In the same time, using the correct superellipsoid parameters ensures that we capture most of the irregularities present over the measured of the corneal surface. We determined that higher superellipsoid parameters that were able to provide a better model fit, but it was also susceptible to noise.

For smooth continuity in the representation of the measured data, a mathematical procedure was developed for interpolating the locations where no measurement had been taken. At locations where no measurement has been taken, the corresponding locations are obtained by interpolation at neighbouring points. In addition, the interpolated values are constrained to be no greater than the measured values.

As an evaluation of the measurement technique, the algorithm was tested.

### IV. CONCLUSIONS

In the context of corneal surface, models and simulations are used to examine the function, structure and nonlinear dynamics as an accurate and rigorous tool for generating quantitative and qualitative predictions.

Mathematical analysis of corneal models is often restricted to special cases with particular features. Numerical simulations can expand the range and allow understanding how analysis of the special cases relates to more realistic situations.

In this paper are proposed contributions concerning in determination of a new mathematical and graphical model using the superellipsoids for the corneal surface, with particular parameters for different subjects (women and men).

The determined parameters for the approximation of human corneal surface with superellipsoids are:

$$a_1 = a_2 = a_3 = 1; \varepsilon_1 = 1, \varepsilon_2 = 0.8 \dots 1.8.$$

This analysis predict that the radius and asphericity of the vertical and horizontal meridians of individual subjects differ. As predicted by the analysis the anterior surface of the cornea becomes more curved with age, but more so in the horizontal meridian than in the vertical meridian.

The radii of both anterior and posterior corneal surfaces and asphericity of anterior corneal surface are not significantly age-dependent, but the asphericity of the posterior corneal surface is age-dependent.

There is a stronger relationship between posterior asphericity and anterior asphericity of the cornea.

These results provide the possibility of optimizing the refractive surgery by considering a new mathematical and CAD graphical model for the corneal surface.

In future improvement of the proposed model, deformable surface and advanced techniques for surface extraction will be chosen.

## REFERENCES

1. Saragoussi J J, Arne J L, Colin J, Montard M (2001) Chirurgie réfractive. Masson, Paris
2. Anera R G, Jimenez J R, Jimenez L B, Diaz J A (2002) Corneal asphericity on visual function after refractive surgery. *Optik* 113 (2): 83–88
3. Guillou M, Lydon D P, Wilson C (1986) Corneal topography: a clinical model. *Ophthal Physiol Opt* 6: 47–56
4. Carroll J P (1994) A method to describe corneal topography. *Optom Vis Sci* 71: 259–264
5. Carney L G, Mainstone J C, Henderson B A (1997) Corneal topography and myopia. A cross-sectional study. *Invest Ophthalmol Vis Sci* 38: 311–320
6. Langenbucher A, Viestenz A, Seitz B (2002) Conoidal fitting of corneal topography height data after excimer laser penetrating keratoplasty. *J Refract Surg* 18: 63–70
7. Kasprzak H T, Jankowska-Kuchta E (1996) A new analytical approximation of corneal topography. *J Modern Opt* 43: 1135–1148
8. Buehren T, Lee BJ, Collins MJ, Iskander DR (2002) Ocular micro-fluctuations and videokeratoscopy. *Cornea* 21: 346–351
9. Buehren T, Collins M J, Iskander D R, Davis B, Lingelbach B (2001) The stability of corneal topography in the post-blink interval. *Cornea* 20: 826–33
10. Zhu M, Collins M J, Iskander D R (2007) Dynamics of ocular surface topography. *Eye* 21: 624–632
11. Kiely P M, Smith G, Carney L G (1982) The mean shape of the human cornea. *Optica Acta* 29: 1027–1040
12. Mainstone J C, Carney L G, Anderson C R, Clem F M, Stephensen A L, Wilson M D (1998) Corneal shape in hyperopia. *Clin Exp Optom* 3: 131–137
13. Sheridan M, Douthwaite WA (1989) Corneal asphericity and refractive error. *Ophthal Physiol Opt* 9: 235–238
14. Patel S, Marshall J, Fitzke E W (1993) The shape and radius of the posterior corneal surface. *Refract Corneal Surg* 9: 173–181
15. Dubbelman M, Weeber H A, Van der Heijde R G, Volker-Dieben H J (2002) Radius and asphericity of the posterior corneal surface determined by corrected Scheimpflug photography. *Acta Ophthalmol Scand* 80: 379–383
16. Mandell RB, St Helen R (1971) Mathematical model of the corneal contour. *Br J Physiol Opt* 26: 185–197
17. Burek H, Douthwaite W (1993) Mathematical models of the general corneal surface. *Ophthal Physiol Opt* 13: 68–72
18. Kasprzak H T, Iskander D R (2006) Approximating ocular surfaces by generalized conic curves. *Ophthal Physiol Opt* 26: 602–609
19. Iskander D R, Collins M J, Davis B (2001) Optimal modeling of corneal surfaces with Zernike polynomials. *IEEE Trans Biomed Eng* 48: 87–95
20. Iskander D R, Morelande M R, Collins M J, Davis B (2002) Modeling corneal surfaces with radial polynomials. *IEEE Trans Biomed Eng* 49: 320–328
21. Lotmar W (1971) Theoretical eye model with aspherics. *J Opt Soc Am* 61: 1522–1529
22. Jaklic A, Leonardis A, Solina F (2000) Segmentation and Recovery of Superquadric. Computational imaging and vision. Kluwer Academic Publishers, Dordrecht, The Netherlands
23. Velho L, Gomes J, Figueiredo L H (2002) Implicit Objects in Computer Graphics. Springer-Verlag, New York, Inc.
24. Chevalier L, Jaillet F, Baskurt A (2003) Segmentation and superquadric modeling of 3D objects. *Journal of Winter School of Computer Graphics, WSCG'03*, 11 (2): 232–239
25. Talu S D, Talu S, Talu M, Shah R (2007) CAD of human corneal surface using new mathematical models. *Acta Electrotehnica of the Technical University of Cluj-Napoca, Romania*, 48 (4): 299–302
26. Wolfram CDF Player 8.0.1.0 by Wolfram Research, Inc., 100 Trade Center Drive Champaign, IL 61820-7237 USA, 1988–2011, at <http://www.wolfram.com/cdf-player>.
27. Kragler R, Superquadrics from the Wolfram Demonstrations Project, at <http://demonstrations.wolfram.com/Superquadrics/>
28. You S, Neumann U (1998) Automatic Object Modeling for 3D Virtual Environment, International Workshop on Non-linear Model Based Image Analysis, Scotland
29. Bhabhrwala T (2004) Shape recovery from medical image data using Extended superquadrics. Doctoral thesis, Buffalo, New York, USA.
30. Levenberg K (1944) A method for the solution of certain problems in least squares. *Quarterly Applied Mathematics* 2: 164–168
31. Marquardt D (1963) An algorithm for least squares estimation of nonlinear parameters. *SIAM Journal of Applied Mathematics* 11: 431–441
32. Moré J J (1977) The Levenberg-Marquardt Algorithm: Implementation and Theory, Numerical Analysis. Ed. G. A. Watson, Lecture Notes in Mathematics 630, Springer Verlag

Author: Mihai Talu

Institute: Faculty of Mechanics / Department of Applied Mechanics,  
University of Craiova, Romania  
Street: Calea Bucuresti Street, no. 165  
City: Craiova  
Country: Romania  
Email: mihai\_talu@personal.ro